Antagonistic evolution of an antibiotic and its molecular chaperone: how to maintain a vital ectosymbiosis in a highly fluctuating habitat

Claire Papot, François Massol, Didier Jollivet, Aurélie Tasiemski

SUPPLEMENTARY INFORMATION

EXTENDED EXPERIMENTAL PROCEDURES

Gene amplification. The preproalvinellacin gene displays a 5 introns/6 exons structure, with a first large intron of 449 bp after the signal peptide sequence [1] (Fig. 2). Because of its length, nested primers with a 100 bp overlap in the middle of the gene were designed to split the gene at the beginning of the BRICHOS domain (see table S1): the 5' part comprises both the peptide signal and the linker region (3 exons + 3 introns) whereas the 3' part contains the BRICHOS domain and the antimicrobial peptide (3 exons + 2 introns).

Specimen sampling

The genus *Alvinella* is made of only two species: the Pompeii worm *A. pompejana* and its closely related syntopic species *A. caudata*. Both species live on the wall of vent chimneys distributed along the East Pacific Rise (EPR). Animals were collected using the arm of the manned submersible Nautile and brought back to the surface inside an insulated basket. Until sampled, animals were measured, sexed and frozen immediately at -80°C for further laboratory analysis or alternatively freshly dissected to perform a DNA extraction directly onboard from the anterior part of the animal (gills and prostomium, which are devoid of epibionts). The two sampling sites are separated by a distance of about 3000km and a major faulting system (Quebrada/Discovery/Gofar fracture zone) around the Equator known to represent a biogeographic barrier for the vent fauna [2]. *Alvinella* specimens from both sides of the EPR therefore display a *Cox-1* specific mitochondrial signature with 2% divergence.

PCR amplification, cloning and sequencing

Four *A. caudata* specimens and 96 *A. pompejana* were sampled from populations on both sides of the Equatorial barrier (50 individuals from Fromveur and 50 individuals from Bio9). Each individual was amplified by PCR separately with a different tag combination. PCR were conducted in a 25µL volume including: 1X buffer, 2mM MgCL2, 0.05mM of each dNTP, 0.4µM of each primer, 1U of Taq polymerase (Uptitherm^{TM}, Interchim). Thermal cycling parameters used an initial denaturation step at 96°C for 4 min, followed by 40 cycles at 96°C for 30 s, 60°C for 45 s and 72°C for 2 min, before a 10 min final extension at 72°C. PCR products were then pooled together before cloning. In *A. pompejana*, the technique consisted in pooling the same amount of DNA from PCR amplification of 16 previously tagged individuals for each cloning assay and, to perform six distinct cloning assays for both the 5' and 3' regions of the gene. In other words, 12 pools were made representing 96 individuals for each part of the gene (i.e. 192 amplifications representing 384 allelic fragments for an autosomal locus). Pools of tagged PCR products were purified using QIAquick^{TM} columns and ligated into a Bluescript vector using the TOPO_TA cloning kit (Invitrogen^{TM}) and subsequently transformed into top10 competent *E. coli* strain following the manufacturer's instructions. For each cloning assay, after amplification of the insert with Puc-specific plasmid (outside the polyclonal region) BS1 primers, 96 positive clones (i.e. containing an insert of the right size) were sequenced on both strands with the sequencing primers M13F or M13R, leading to a total number of 1152 sequences and a recapture effort of 3.0 under the single locus assumption. The mark-recapture cloning method led to more than 900 proof-read sequences in both directions (321 in the 5' region and 566 in the 3' region) for the focus species *A. pompejana* and only 20 and 58 sequences in the 5' and 3' regions for the outgroup species *A. caudata*. A consensus sequence of the two forward and reverse reads was produced for each clone. Sequences recaptured more than once were the only sequences kept for the first allelic assignment to duplicated loci. The mark-recapture cloning technique generates about 30% of artifactual recombinants with our complex dataset when looking at the most recaptured individuals (c.a. > 20 clones). These chimeric alleles were either due to intra-locus or inter-loci recombination during the PCR. Some recombinants were, however, considered to be natural when recaptured in more than two individuals (i.e. alleles with the same recombination breakpoints in distinct individuals).

Cleaning sequence datasets from artifactual mutational events

Global alignments of consensus sequences were obtained with the Geneious software using ClustalW with the free ends gap option, a gap penalty of 1.0 and a cost matrix option of 51% similarity. Chimeras of alleles for heterozygous individuals or chimeras of alleles between closely-related loci in the specific case of duplicated genes were of frequent occurrences in our sequence datasets. Tracing back recombinants was, however, only possible for the most recaptured individuals displaying at least 20 clones mainly because of the high number of duplicated genes in our set of sequences. Hence, intra-individual *in vitro* recombination points between alleles and/or duplicated genes were searched using RDP4.0. First, for each set of clonal sequences attributed to one individual, the alignment-based “Automated MAxChi” procedure [3] was performed with all settings left as default. The within-individual alignment with ‘true’ allelic sequences and identified chimeras was thereafter checked manually to visualize any additional intra-individual recombinants. Second, putative recombinants in a given individual were compared with the whole sequence dataset to see whether they might be shared with other individuals. Recombinants found in more than one individual were kept and assumed to represent ‘natural’ intra- or inter-loci recombination events. Third, a second set of recombinant search was performed with the MAxChi procedure over the multi-individual alignment of the remaining sequences to identify additional recombining points across distinct individuals. These new recombinants were also removed from the dataset if not observe in at least two distinct individuals. This allowed us to confirm the natural existence of previously described alleles. Finally, alleles from individuals weakly recaptured or only recaptured once were added to the final dataset if they were able to match at least one sequence of the curated alignment. On this ‘cleaned’ dataset, artifactual/somatic mutations were also removed taking advantage of the multiple recaptures (i.e. >20 sequences) by suppressing singletons between intra-individual sequences that referred to a well-assigned allele. This allowed us to calculate a rate at which artifactual mutations occur in the dataset and to apply this rate on singletons found in the other less recaptured individuals.

Paralog identification and individual genotyping

Combining the 5’ and 3’ regions of the gene (separate PCR amplification) and thus, the exact correspondence of 5’ and 3’ alleles, was not possible in this study due to the high rate of recombination and the lack of diagnostic sites in the 100 bp-overlapping region of the gene, leading to a disjoint assignment of paralogs in the two genic regions. Exact allelic concordance was only met for 5’ paralog 5 and the 3’ paralog E as they both display the highest level of divergence with the other paralogs, respectively. A detailed analysis of paralogs was performed at the intraspecific level from the whole ‘cleaned’ sequence dataset recovered from *A. pompejana* on the 5’ region of the gene. This region was chosen because it contains long intronic regions that help to discriminate more easily between paralogs (i.e. specific signatures of linked sites). Forward and reverse paralog-specific primers were positioned on specific mutation signatures typifying each putative paralog with a final amplicon size of less than 400-nucleotides long. For each paralogous gene, direct sequencing allowed us to search for heterozygous individuals (double peaks in the chromatogram) at diagnostic sites using an alignment performed with the *de novo* Assemble module of the Geneious software. Gene orthology was confirmed for a given set of primers when both homozygous and heterozygous individuals co-occur at previously chosen diagnostic sites.

The evolutionary history of paralogs was inferred with the Maximum Likelihood method of the software MEGA6 using the GTR model of substitutions and the allelic alignment of either the 5’ or 3’ regions (coding and non-coding region) of the gene. Initial tree(s) for the heuristic search were obtained by applying the BioNJ method to a matrix of pairwise distances estimated using the Maximum Composite Likelihood (MCL) approach. A discrete Gamma distribution was used to model evolutionary rate differences among sites (4 categories (Gamma shape parameter = 0.13) with no invariable sites). The tree was drawn to scale with branch lengths measured as the number of substitutions per site. A search for the best model of substitutions was also performed using jModelTest 2.1.7. The tree topology obtained with the GTR+I+G model was compared with possible alternative trees. Results using the whole set of allelic sequences of the 5’ region of the gene indicated that the best substitution model is the GTR+G according to the AIC or the TPM3uf+G model according to the BIC, but the three models (GTR+I+G, GTR+G and TPM3uf+G) fall within the 95% confidence intervals of the AIC/BIC analyses (i.e. models which have a substantial support for the dataset by summing the ranked weight (ωi) of each model (i) that uses the difference between each model-specific value of AIC/BIC and the minimum one). There was no significant difference between the GTR+G and GTR+G+I models (LRT=2.22, df=1) and the TPM3uf model produced a significantly decreased likelihood than the GTR+G+I model (LRT=2.45, df=4). Comparing the topologies obtained with PhyML under the two selected best models and the GTR+G+I model did not give much difference in topology (see alternative topologies below). Slight differences in the coalescence of alleles within each paralog were observed but were not taken into account, as they have no influence on the arrangement of clades.

The phylogenetic network constructed via the NeighborNet method implemented in the program SplitsTree4 [4] indicated that the preproalvinellacin is encoded by a multigenic family of six genes (par1, par2, par3a, par3b, par4 and par5), some of the alleles being recently derived recombinants (Par5 R2) while others (Par5 R1, Par4-1 R) represent older recombinants that have already accumulated their proper set of mutations. Twelve unambiguous sequences were kept for par1, 6 for par2, 13 for par3a, 9 for par3b, 14 for par4 and 25 for par5. The length of alleles dramatically varied between paralogs, mainly because of indels in the intronic regions. No indel was depicted in the exonic regions with the exception of Par2 which lacks a piece of 34 codons located at the end of the first exon and the beginning of the second one without changing the reading frame. Par4 displayed the lowest length due to a major deletion in the first intronic region. Par5 was the most divergent lineage mainly because of the first intron, which exhibited a tandem repeat region and could not be aligned with the other sequences (foreign insertion due to an unequal crossing over with another gene).

Strength of selection along the preproalvinellacin gene

Intensity of selection acting on each domain of the gene (i.e. signal peptide, propiece, BRICHOS and AMP) according to each paralog was measured using the ratio of non-synonymous substitution rate (d_N), which are usually subject to selective pressure, and the synonymous substitution rate (d_S), which is assumed to be (nearly) neutral [5,6]. Values greater than one were assumed to show positive diversifying selection on the divergence between two paralogous domains, and thus positive diversification of duplicates.

Search for positive selection in the propiece and BRICHOS regions of preproalvinellacin

Paralogous consensus sequences of the propiece (79 sequences) and the BRICHOS plus the alvinellacin AMP (36 sequences) were aligned together using ClustalW of the alignment module of Geneious for *A. pompejana* and *A. caudata*. All positions with less than 95% site coverage were eliminated, leading to a total of 681 site positions in the final dataset. A search for the best model of substitutions was performed with jModelTest 2.1.7 and the tree topologies obtained from the PhyML reconstruction with these models were compared to the topology obtained with the GTR+I+G, as implemented in MEGA6 (Tables S2 and S3). Using the BRICHOS alignment, a hLRT backward selection procedure showed that none of the nested substitution models had significantly poorer goodness-of-fit than the GTR+I+G model (log likelihood=-439.625, BIC=1299.380) with the exception of the JC+I+G model (log likelihood= -452.175). Because the best model was the K80+I according to the BIC (log likelihood=-441.781, BIC=1261.15), we carefully examined the topology of the BIC-based best tree when compared to the GTR+I+G used for CodeML and aaML analyses (Fig. S3). Though more simplistic, the K80+I topology between the paralogous clades was not different from the one given by the GTR+I+G model and thus does not affect either the ancestral reconstruction or the search for positive selection on codons. For the propiece CodeML analysis (79 sequences), the AIC-based best model was also the K80+I model (log likelihood=-607.94, AICc= 3657.6) but the TPM2+I+G model (log likelihood=-588.29, BIC=1997.1) according to the BIC. Both models had better goodness-of-fit criteria than the GTR+I+G model (log likelihood=-579.8, AICc=5402.5, BIC=2016.5). However, hLRTs in backward selection indicated no significant differences in goodness-of-fit between nested models until the Tim2ef+I+G model. Tree reconstruction with this specific model did not modify the topology of the reference tree used for the Propiece analyses. Models H80+I and Tim2ef+I+G were then used for the tree reconstruction of a smaller set of duplicate-specific consensus sequences for either the BRICHOS or the Propiece domain (8 sequences each) and, subsequently used in the CodeML analyses for the article in order to remove polymorphic sequences from the analysis (Figs S3 and S4). Results from the small sets of consensus sequences are now provided in Table 2 and results from all sets of sequences (including polymorphic ones) are provided in Tables S6 and S7. Several nested models of codon selection (i.e. M_3, M_{2a} and M_8) were subsequently tested against their ‘nearly neutral’ counterparts (i.e. M_0, M_{1a} and M_7, respectively) using a likelihood ratio test (LRT). The codon sequence dataset was first fitted on the 'nearly neutral' model M_{1a}, which divides codon sites into two categories, those under purifying selection ($\omega_0<1$) and the others under relaxed selection ($\omega_1=1$) using our reference tree. This model was then compared to the alternative nested 'selection' model M_{2a} where a third category of codon sites under positive selection ($\omega_2>1$) is added, thus accommodating positively selected sites. More sophisticated alternative nested models - the 'nearly neutral beta' M_7 and the 'selective beta' M_8 - were also compared. These models assume an omega distribution that follows a β (p,q) distribution with the shape parameter estimated in the interval [0, 1]. The difference between the two nested models lies in the fact that M_8 includes one additional substitution rate ω_1 with a probability p_1 that accounts for positively selected sites. In these two models, the rate of synonymous substitutions (d_S) is fixed among sites, while the rate of non-synonymous substitutions (d_N) remained variable along the gene. The significance of selection models using a likelihood ratio test with a degree of freedom equal to the difference between the number of parameters estimated for the 2 models when comparing M_{2A} vs. M_{1A} and, M_8 vs. M_7 (adapted from [7]).

MacDonald-Kreitman test between pairs of paralogs

Another approach to detect signs of positive selection, the MacDonald-Kreitman test, was also performed onto the propiece and BRICHOS regions of the *preproalvinellacin* taking advantage of the fixed divergence between paralogs. Under strict neutrality, both rates of synonymous and non-synonymous substitutions are expected to be equal in either the species divergence or the within-species polymorphisms, but d_N/d_S would become much greater than p_N/p_S under positive diversifying selection. None of the tests was significant but MK test can be easily biased if the constancy of the neutral accumulation of mutations is not met over time for duplicates [8]. In order to test whether selective relaxation has occurred prior to the duplication events, we performed a Branch model analysis with CodeML by comparing the ‘free ratio’ model M_1 to the ‘one ratio’ model M_0 and checked whether the d_N/d_S ratios were higher in the internal branches leading to the duplicates when compared to their associated terminal branches. For the BRICHOS domain, M_1 (log likelihood=-370.654, np=29) was not significantly better (LRT=9.44, df=13, NS) than M_0 (log likelihood=-375.374, np=16), with a nearly neutral evolution before and after duplication (overall omega=0.64). For the Propiece domain, M_1 (log likelihood=-396.573, np=29) was also not significantly better (LRT=19.84, df=13, NS) than M_0 (log likelihood=-406.491, np=16), but its evolution was even more relaxed with positive selection (overall omega=1.18). In this case, terminal branches (6 out of eight with omega>1 for the Propiece) produced much higher d_N/d_S ratios than their internal counterparts when using the M_1 branch-model.

SUPPLEMENTARY FIGURES AND TABLES

Figure S1. BRICHOS and alvinellacin amino-acid alignment. Sequence labels represent the individual and clone number and are representative of the 6 paralogous clades (excluding natural recombinants, see Fig. 2) subsequently used in the mapping of the BRICHOS mutations. Ac: *A. caudata*; Ap *A. pompejana*

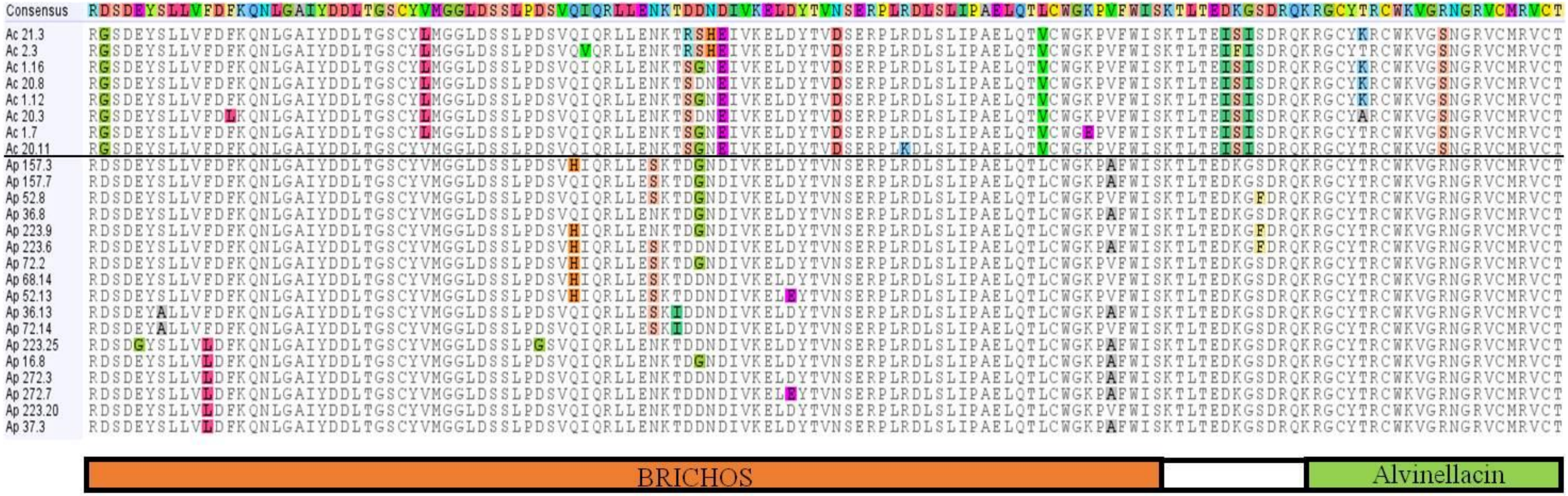

```
Consensus  RDSDEYSLLVFDFKQNLGAIYDDLTGSCYVMGGLDSSLPDSVQIQRLLENKTDDNDIVKELDYTVNSERPLRDLSLIPAELQTLCWGKPVFWISKTLTEDKGSDRQKRGCYTRCWKVGRNGRVCMRVCT
Ac 21.3    RGSDEYSLLVFDFKQNLGAIYDDLTGSCYLMGGLDSSLPDSVQIQRLLENKTRSHEIVKELDYTVDSERPLRDLSLIPAELQTVCWGKPVFWISKTLTEISISDRQKRGCYKRCWKVGSNGRVCMRVCT
Ac 2.3      RGSDEYSLLVFDFKQNLGAIYDDLTGSCYLMGGLDSSLPDSVQVQRLLENKTRSHEIVKELDYTVDSERPLRDLSLIPAELQTVCWGKPVFWISKTLTEIFISDRQKRGCYTRCWKVGSNGRVCMRVCT
Ac 1.16     RGSDEYSLLVFDFKQNLGAIYDDLTGSCYLMGGLDSSLPDSVQIQRLLENKTSGNEIVKELDYTVDSERPLRDLSLIPAELQTVCWGKPVFWISKTLTEISISDRQKRGCYKRCWKVGSNGRVCMRVCT
Ac 20.8     RGSDEYSLLVFDFKQNLGAIYDDLTGSCYLMGGLDSSLPDSVQIQRLLENKTSDNEIVKELDYTVDSERPLRDLSLIPAELQTVCWGKPVFWISKTLTEISISDRQKRGCYKRCWKVGSNGRVCMRVCT
Ac 1.12     RGSDEYSLLVFDFKQNLGAIYDDLTGSCYLMGGLDSSLPDSVQIQRLLENKTSGNEIVKELDYTVDSERPLRDLSLIPAELQTVCWGKPVFWISKTLTEISISDRQKRGCYKRCWKVGSNGRVCMRVCT
Ac 20.3     RGSDEYSLLVFDLKQNLGAIYDDLTGSCYLMGGLDSSLPDSVQIQRLLENKTSDNEIVKELDYTVDSERPLRDLSLIPAELQTVCWGKPVFWISKTLTEISISDRQKRGCYARCWKVGSNGRVCMRVCT
Ac 1.7      RGSDEYSLLVFDFKQNLGAIYDDLTGSCYLMGGLDSSLPDSVQIQRLLENKTSGNEIVKELDYTVDSERPLRDLSLIPAELQTVCWGEPVFWISKTLTEISISDRQKRGCYTRCWKVGSNGRVCMRVCT
Ac 20.11    RGSDEYSLLVFDFKQNLGAIYDDLTGSCYVMGGLDSSLPDSVQIQRLLENKTSGNEIVKELDYTVDSERPLKDLSLIPAELQTVCWGKPVFWISKTLTEISISDRQKRGCYTRCWKVGSNGRVCMRVCT
Ap 157.3    RDSDEYSLLVFDFKQNLGAIYDDLTGSCYVMGGLDSSLPDSVHIQRLLESKTDGNDIVKELDYTVNSERPLRDLSLIPAELQTLCWGKPAFWISKTLTEDKGSDRQKRGCYTRCWKVGRNGRVCMRVCT
Ap 157.7    RDSDEYSLLVFDFKQNLGAIYDDLTGSCYVMGGLDSSLPDSVQIQRLLESKTDGNDIVKELDYTVNSERPLRDLSLIPAELQTLCWGKPAFWISKTLTEDKGSDRQKRGCYTRCWKVGRNGRVCMRVCT
Ap 52.8     RDSDEYSLLVFDFKQNLGAIYDDLTGSCYVMGGLDSSLPDSVQIQRLLESKTDGNDIVKELDYTVNSERPLRDLSLIPAELQTLCWGKPVFWISKTLTEDKGFDRQKRGCYTRCWKVGRNGRVCMRVCT
Ap 36.8     RDSDEYSLLVFDFKQNLGAIYDDLTGSCYVMGGLDSSLPDSVQIQRLLENKTDGNDIVKELDYTVNSERPLRDLSLIPAELQTLCWGKPAFWISKTLTEDKGSDRQKRGCYTRCWKVGRNGRVCMRVCT
Ap 223.9    RDSDEYSLLVFDFKQNLGAIYDDLTGSCYVMGGLDSSLPDSVHIQRLLENKTDGNDIVKELDYTVNSERPLRDLSLIPAELQTLCWGKPVFWISKTLTEDKGFDRQKRGCYTRCWKVGRNGRVCMRVCT
Ap 223.6    RDSDEYSLLVFDFKQNLGAIYDDLTGSCYVMGGLDSSLPDSVHIQRLLESKTDDNDIVKELDYTVNSERPLRDLSLIPAELQTLCWGKPAFWISKTLTEDKGFDRQKRGCYTRCWKVGRNGRVCMRVCT
Ap 72.2     RDSDEYSLLVFDFKQNLGAIYDDLTGSCYVMGGLDSSLPDSVHIQRLLESKTDGNDIVKELDYTVNSERPLRDLSLIPAELQTLCWGKPVFWISKTLTEDKGSDRQKRGCYTRCWKVGRNGRVCMRVCT
Ap 68.14    RDSDEYSLLVFDFKQNLGAIYDDLTGSCYVMGGLDSSLPDSVHIQRLLESKTDDNDIVKELDYTVNSERPLRDLSLIPAELQTLCWGKPVFWISKTLTEDKGSDRQKRGCYTRCWKVGRNGRVCMRVCT
Ap 52.13    RDSDEYSLLVFDFKQNLGAIYDDLTGSCYVMGGLDSSLPDSVHIQRLLESKTDDNDIVKELEYTVNSERPLRDLSLIPAELQTLCWGKPVFWISKTLTEDKGSDRQKRGCYTRCWKVGRNGRVCMRVCT
Ap 36.13    RDSDEYALLVFDFKQNLGAIYDDLTGSCYVMGGLDSSLPDSVQIQRLLESKIDDNDIVKELDYTVNSERPLRDLSLIPAELQTLCWGKPAFWISKTLTEDKGSDRQKRGCYTRCWKVGRNGRVCMRVCT
Ap 72.14    RDSDEYALLVFDFKQNLGAIYDDLTGSCYVMGGLDSSLPDSVQIQRLLESKIDDNDIVKELDYTVNSERPLRDLSLIPAELQTLCWGKPVFWISKTLTEDKGSDRQKRGCYTRCWKVGRNGRVCMRVCT
Ap 223.25   RDSDGYSLLVLDFKQNLGAIYDDLTGSCYVMGGLDSSLPGSVQIQRLLENKTDDNDIVKELDYTVNSERPLRDLSLIPAELQTLCWGKPAFWISKTLTEDKGSDRQKRGCYTRCWKVGRNGRVCMRVCT
Ap 16.8     RDSDEYSLLVLDFKQNLGAIYDDLTGSCYVMGGLDSSLPDSVQIQRLLENKTDGNDIVKELDYTVNSERPLRDLSLIPAELQTLCWGKPAFWISKTLTEDKGSDRQKRGCYTRCWKVGRNGRVCMRVCT
Ap 272.3    RDSDEYSLLVLDFKQNLGAIYDDLTGSCYVMGGLDSSLPDSVQIQRLLENKTDDNDIVKELDYTVNSERPLRDLSLIPAELQTLCWGKPAFWISKTLTEDKGSDRQKRGCYTRCWKVGRNGRVCMRVCT
Ap 272.7    RDSDEYSLLVLDFKQNLGAIYDDLTGSCYVMGGLDSSLPDSVQIQRLLENKTDDNDIVKELEYTVNSERPLRDLSLIPAELQTLCWGKPAFWISKTLTEDKGSDRQKRGCYTRCWKVGRNGRVCMRVCT
Ap 223.20   RDSDEYSLLVLDFKQNLGAIYDDLTGSCYVMGGLDSSLPDSVQIQRLLENKTDDNDIVKELDYTVNSERPLRDLSLIPAELQTLCWGKPVFWISKTLTEDKGSDRQKRGCYTRCWKVGRNGRVCMRVCT
Ap 37.3     RDSDEYSLLVLDFKQNLGAIYDDLTGSCYVMGGLDSSLPDSVQIQRLLENKTDDNDIVKELDYTVNSERPLRDLSLIPAELQTLCWGKPAFWISKTLTEDKGSDRQKRGCYTRCWKVGRNGRVCMRVCT
```

Figure S2. Tree topology comparisons between GTR+I+G and the AIC- and BIC-based best models for the most variable 5' region of the preproalvinellacin used in the identification of paralogous genes. Comparison between topologies of the alvinellacin paralogous MEGA tree obtained in Figure 2 using (**A**) the GTR+I+G model implemented in MEGA 6.0 (log likelihood= 5367.044, AIC=14030.71, BIC=14981.24), (**B**) the selected best model (GTR+G) obtained with jModelTest v2.1.7 based on the AIC criterion (log likelihood=-5365.93, AIC=14025.04) and, (**C**) the selected best model (TPM3uf+G) obtained with jModelTest v2.1.7 based on the BIC criterion (log likelihood=-5368.27, BIC=14963.74). Note that these three models fall within the 95% confidence intervals of the jModelTest analysis, and that the three models are not significantly different according to hierarchical likelihood ratio tests (LRT). Slight differences can be observed in the gene genealogies of each paralogous clade but do not affect the clade rearrangement.

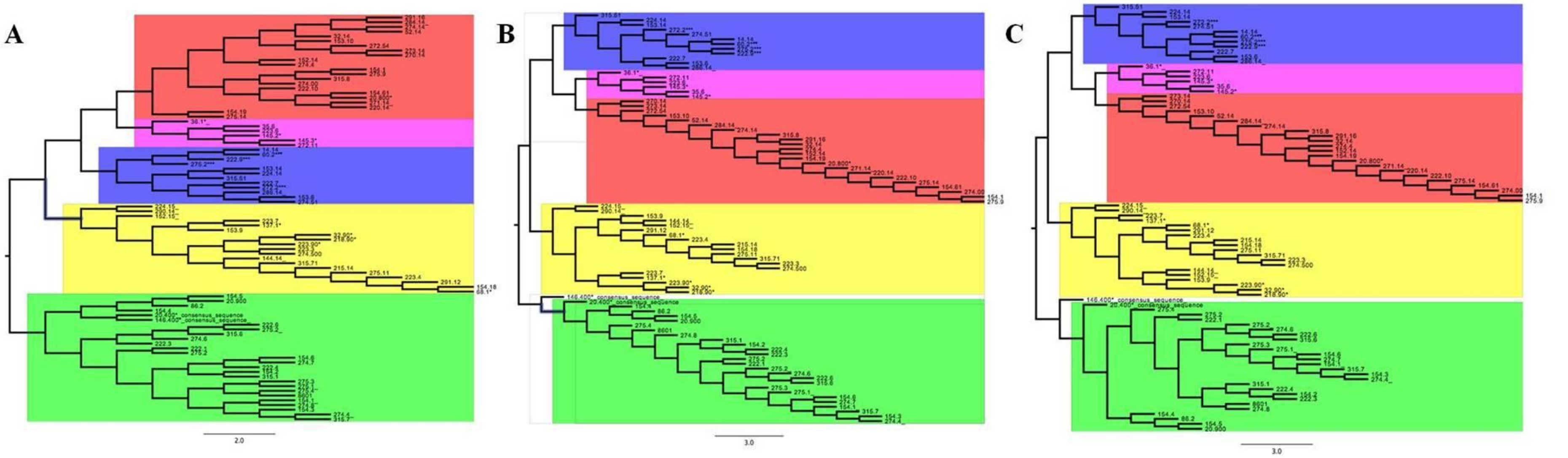

Fig. S3. PhyML tree of the BRICHOS domain using the K80+I model selected by jmodeltest according to the BIC. Topology of BRICHOS trees obtained using the K80+I model selected by jModelTest 2.1.7 according to the BIC criterion (log likelihood=-441.781, BIC=1261.15). This tree topology was not different from the one obtained using the GTR+I+G model implemented in MEGA 6.0 (Fig. 4 in main text) and led to the exact same conclusions when used as the reference tree in the CodeML and aaML analyses.

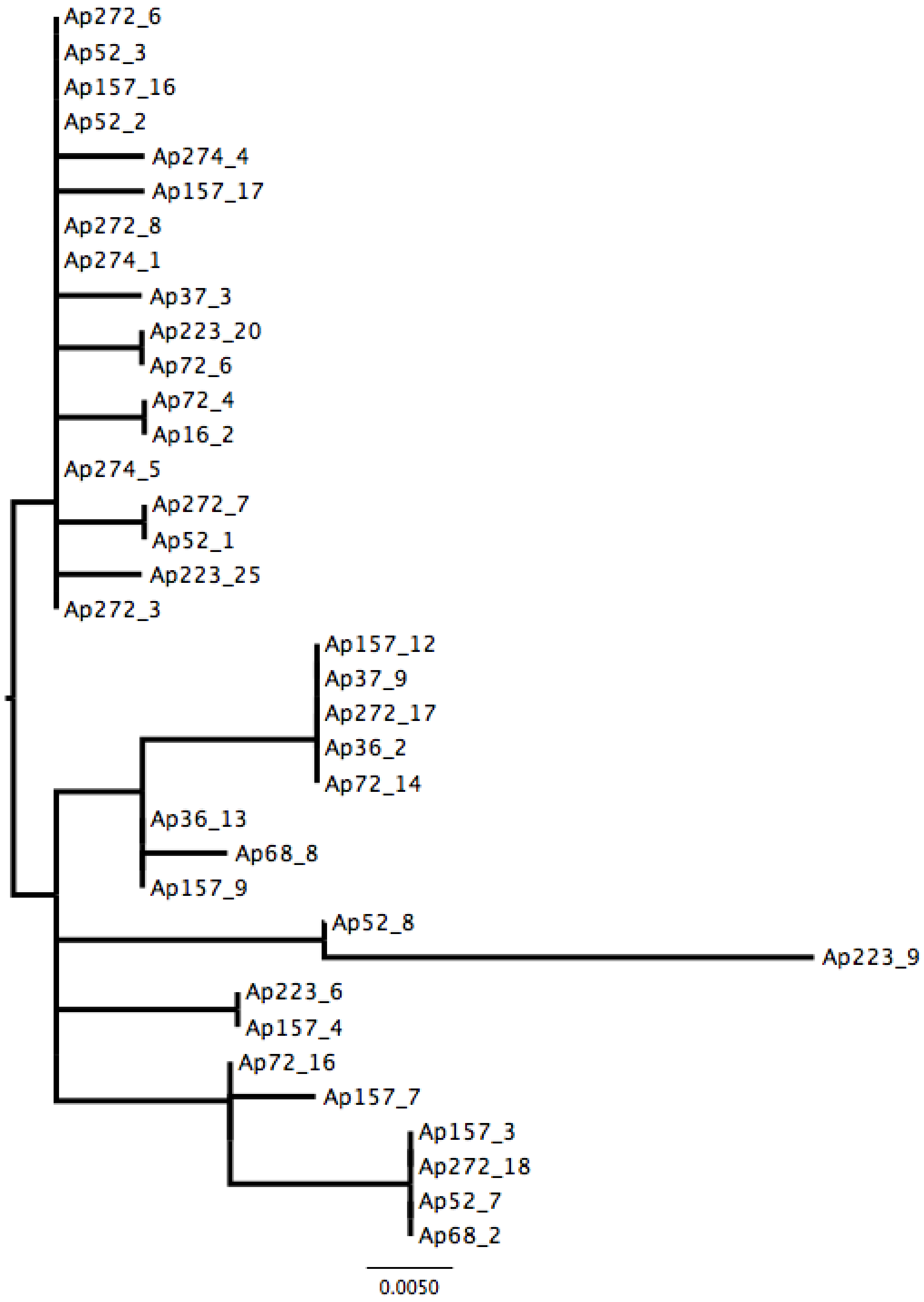

Fig. S4. Propiece ML tree topology using the GTR+I+G model implemented in MEGA 6.0 and the BIC-based best model (TPM2ef+I+G) obtained from the jModelTest analysis. Both models led to the same topology and all the 88 substitution models tested fall within the 95% confidence interval of the AIC/BIC analyses (see text). (**A**) Ultrametric and (**B**) chronogram representations of the same tree topology.

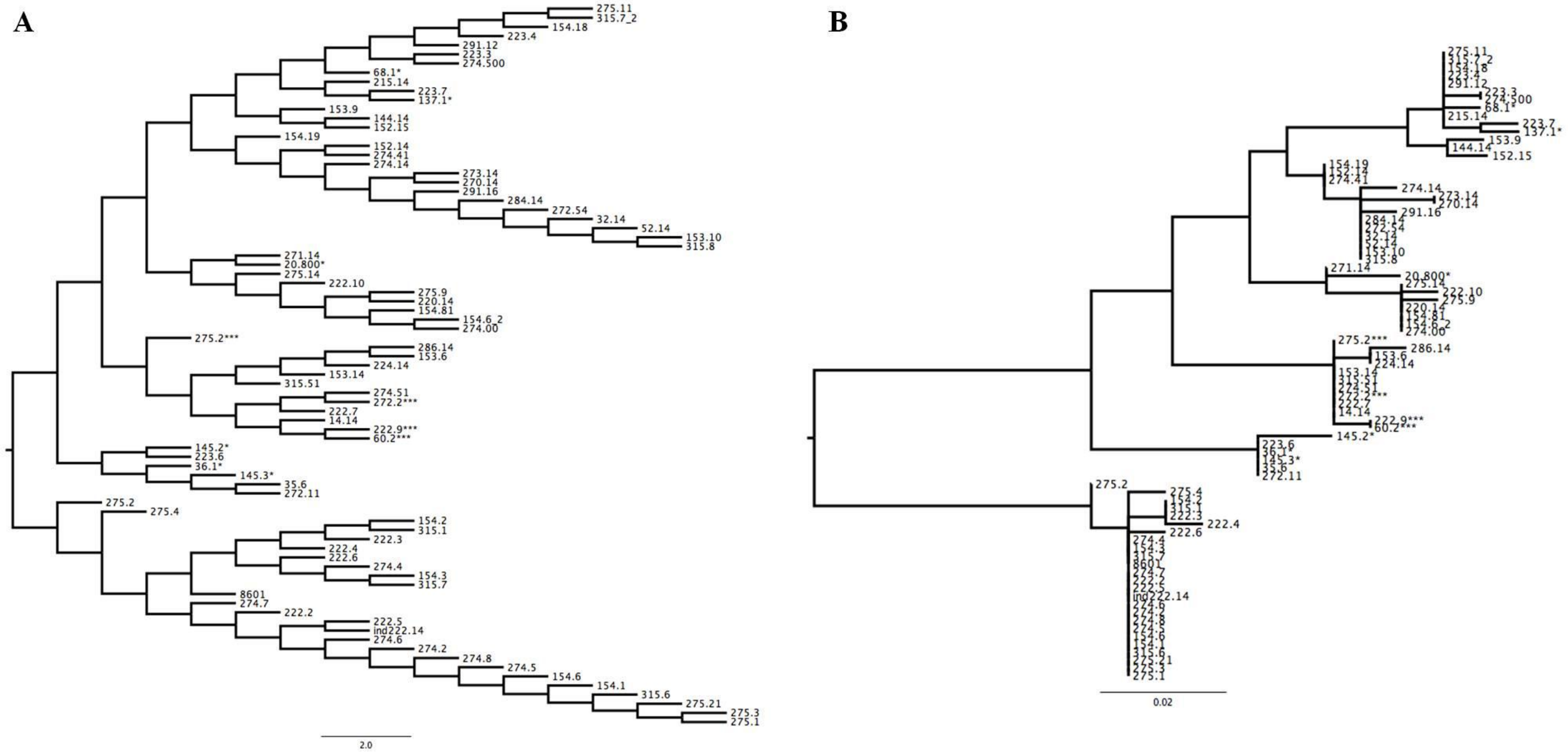

Table S1. Primers sequences (Forward and Reverse) used for the amplification of the preproalvinellacin gene from both *Alvinella pompejana* and *Alvinella caudata* and used for the genotyping of each paralogs (Px) for the *Alvinella pompejana* species.

Alvinella pompejana		
	3' Forward	ATCGTGTTACGTCATGGGTGGCCTTG
	3' Reverse	CTCAGTGAAATGAAGCAGGTGAGTTATG
	5' Forward	ATGACGTATTCTGTAGTTGTGACGCTGGTC
	5' Reverse	ATCCGGTAAGATCGTCGTAAATGGCTCC
Genotyping		
	P1_Forward	ACATCTACAGATTGGTGCTATCGAC
	P2_Forward	CTACAGATTGGTGCAGCCGAC
	P3_Forward	CATCTACAGATTGGTGCTGTGGAT
	P4_Forward	AACAGATTGGTGCTGTCGCC
	P5_Forward	TTTACATAGATTGGTGTTTCTTCTCTGAG
	P1_Reverse	GTTGAGGTGGCCAGCTGC
	P2-Reverse	GTTGGGGTGGCCAACTGC
	P3_Reverse	ATGTTGGGGTGATCAGCTGC
	P4_Reverse	GATGTTGAGGTGGCCAGCTAT
	P5_Reverse	GTTTCATGAAATGTGGCAGATG
Alvinella caudata		
	5' Forward	GTTACGTATTCTGTAGTCACGACGCTG
	5' Reverse	GGTAAGATCGTCGTAAATGGCTCC
	3' Forward	GTCGTGTTACCTGATGGGTGGC
	3' Reverse	AATATGCCAAAACAGGCGAATTACG

Table S2. AIC-based goodness-of-fit indicators of substitution models for the most variable 5’ region of the preproalvinellacin used in the identification of paralogous genes, obtained from jModelTest. Models are ordered by increasing AIC.

Model	**- log likelihood**	**number of parameters**	**AIC**	**ΔAIC**	**Akaike weight**	**Cumulative weight**
GTR+G	6833.52	179	14025.04	0.00	0.75	0.75
TVM+G	6836.38	178	14028.75	3.71	0.12	0.87
GTR+I+G	6835.36	180	14030.71	5.67	0.04	0.92
TIM3+G	6838.39	177	14030.79	5.75	0.04	0.96
TVM+I+G	6836.73	179	14031.46	6.42	0.03	0.99
TPM3uf+G	6841.17	176	14034.33	9.29	0.01	1.00
TIM3+I+G	6840.53	178	14037.07	12.03	0.00	1.00
TPM3uf+I+G	6841.72	177	14037.43	12.39	0.00	1.00
TIM2+G	6842.97	177	14039.95	14.91	0.00	1.00
TPM2uf+G	6844.39	176	14040.79	15.75	0.00	1.00
TrN+G	6847.11	176	14046.22	21.18	0.00	1.00
TIM2+I+G	6845.54	178	14047.08	22.04	0.00	1.00
TPM2uf+I+G	6847.15	177	14048.29	23.25	0.00	1.00
HKY+G	6850.36	175	14050.72	25.68	0.00	1.00
TIM1+G	6848.95	177	14051.90	26.86	0.00	1.00
TPM1uf+G	6850.07	176	14052.15	27.11	0.00	1.00
TrN+I+G	6849.80	177	14053.60	28.56	0.00	1.00
GTR+I	6848.00	179	14054.00	28.96	0.00	1.00
HKY+I+G	6851.19	176	14054.38	29.34	0.00	1.00
TIM1+I+G	6849.49	178	14054.97	29.93	0.00	1.00
TVM+I	6849.67	178	14055.35	30.31	0.00	1.00
TPM1uf+I+G	6850.88	177	14055.76	30.72	0.00	1.00
TIM3+I	6853.24	177	14060.49	35.45	0.00	1.00
TPM3uf+I	6854.83	176	14061.66	36.63	0.00	1.00
TIM2+I	6858.26	177	14070.53	45.49	0.00	1.00
TPM2uf+I	6859.96	176	14071.93	46.89	0.00	1.00
TrN+I	6862.51	176	14077.01	51.97	0.00	1.00
HKY+I	6864.07	175	14078.14	53.10	0.00	1.00
TIM1+I	6862.28	177	14078.57	53.53	0.00	1.00
TPM1uf+I	6863.76	176	14079.51	54.47	0.00	1.00
TPM3+I+G	6870.38	174	14088.76	63.72	0.00	1.00
TIM3ef+I+G	6869.91	175	14089.82	64.78	0.00	1.00
TVMef+I+G	6869.05	176	14090.10	65.06	0.00	1.00
SYM+I+G	6868.59	177	14091.18	66.14	0.00	1.00
TPM3+G	6873.36	173	14092.73	67.69	0.00	1.00
K80+I+G	6873.63	173	14093.25	68.21	0.00	1.00
TPM1+I+G	6872.68	174	14093.36	68.32	0.00	1.00
TIM3ef+G	6872.94	174	14093.88	68.84	0.00	1.00
TIM1ef+I+G	6872.21	175	14094.42	69.38	0.00	1.00
TVMef+G	6872.27	175	14094.54	69.50	0.00	1.00
TrNef+I+G	6873.27	174	14094.55	69.51	0.00	1.00
TPM2+I+G	6873.52	174	14095.05	70.01	0.00	1.00

SYM+G	6871.85	176	14095.69	70.65	0.00	1.00
TIM2ef+I+G	6873.06	175	14096.12	71.08	0.00	1.00
K80+G	6876.61	172	14097.22	72.18	0.00	1.00
TPM1+G	6875.85	173	14097.70	72.66	0.00	1.00
TrNef+G	6876.18	173	14098.37	73.33	0.00	1.00
TIM1ef+G	6875.42	174	14098.84	73.80	0.00	1.00
TPM2+G	6876.54	173	14099.08	74.04	0.00	1.00
TIM2ef+G	6876.12	174	14100.24	75.20	0.00	1.00
TPM3+I	6889.00	173	14123.99	98.95	0.00	1.00
TIM3ef+I	6888.42	174	14124.83	99.79	0.00	1.00
TVMef+I	6887.70	175	14125.40	100.36	0.00	1.00
SYM+I	6887.12	176	14126.24	101.20	0.00	1.00
K80+I	6892.58	172	14129.16	104.12	0.00	1.00
TPM1+I	6891.71	173	14129.42	104.38	0.00	1.00
TIM1ef+I	6891.14	174	14130.29	105.25	0.00	1.00
TrNef+I	6892.23	173	14130.45	105.41	0.00	1.00
TPM2+I	6892.44	173	14130.89	105.85	0.00	1.00
TIM2ef+I	6891.88	174	14131.77	106.73	0.00	1.00
F81+G	6931.81	174	14211.62	186.58	0.00	1.00
F81+I+G	6932.11	175	14214.22	189.18	0.00	1.00
F81+I	6945.08	174	14238.17	213.13	0.00	1.00
TVM	6943.77	177	14241.53	216.49	0.00	1.00
GTR	6943.17	178	14242.33	217.29	0.00	1.00
TPM3uf	6948.84	175	14247.69	222.65	0.00	1.00
TIM3	6948.29	176	14248.57	223.53	0.00	1.00
JC+G	6954.45	171	14250.90	225.86	0.00	1.00
JC+I+G	6955.38	172	14254.76	229.73	0.00	1.00
TPM2uf	6956.76	175	14263.52	238.48	0.00	1.00
TIM2	6956.10	176	14264.19	239.15	0.00	1.00
HKY	6960.49	174	14268.98	243.94	0.00	1.00
TrN	6959.87	175	14269.75	244.71	0.00	1.00
TPM1uf	6960.14	175	14270.28	245.24	0.00	1.00
TIM1	6959.54	176	14271.08	246.04	0.00	1.00
JC+I	6970.40	171	14282.79	257.75	0.00	1.00
TPM3	6987.80	172	14319.61	294.57	0.00	1.00
TVMef	6985.82	174	14319.64	294.60	0.00	1.00
TIM3ef	6987.64	173	14321.27	296.23	0.00	1.00
SYM	6985.65	175	14321.31	296.27	0.00	1.00
TPM1	6991.78	172	14327.57	302.53	0.00	1.00
K80	6993.01	171	14328.01	302.97	0.00	1.00
TIM1ef	6991.59	173	14329.18	304.14	0.00	1.00
TPM2	6992.77	172	14329.54	304.50	0.00	1.00
TrNef	6992.87	172	14329.74	304.70	0.00	1.00
TIM2ef	6992.58	173	14331.15	306.11	0.00	1.00
F81	7034.17	173	14414.33	389.29	0.00	1.00
JC	7061.49	170	14462.99	437.95	0.00	1.00

Table S3. BIC-based goodness-of-fit indicators of substitution models for the most variable 5’ region of the preproalvinellacin used in the identification of paralogous genes, obtained from jModelTest. Models are ordered by increasing BIC.

Model	- log likelihood	number of parameters	AIC	ΔAIC	Akaike weight	Cumulative weight
TPM3uf+G	6841.17	176	14963.74	0.00	0.62	0.62
TIM3+G	6838.39	177	14965.47	1.73	0.26	0.88
TVM+G	6836.38	178	14968.72	4.98	0.05	0.93
TPM2uf+G	6844.39	176	14970.19	6.45	0.02	0.96
GTR+G	6833.52	179	14970.28	6.55	0.02	0.98
TPM3uf+I+G	6841.72	177	14972.12	8.38	0.01	0.99
TIM2+G	6842.97	177	14974.63	10.89	0.00	0.99
HKY+G	6850.36	175	14974.84	11.11	0.00	1.00
TrN+G	6847.11	176	14975.62	11.89	0.00	1.00
TVM+I+G	6836.73	179	14976.70	12.97	0.00	1.00
TIM3+I+G	6840.53	178	14977.03	13.30	0.00	1.00
GTR+I+G	6835.36	180	14981.24	17.50	0.00	1.00
TPM1uf+G	6850.07	176	14981.55	17.81	0.00	1.00
TPM2uf+I+G	6847.15	177	14982.98	19.24	0.00	1.00
HKY+I+G	6851.19	176	14983.79	20.05	0.00	1.00
TIM1+G	6848.95	177	14986.58	22.84	0.00	1.00
TIM2+I+G	6845.54	178	14987.04	23.31	0.00	1.00
TrN+I+G	6849.80	177	14988.28	24.55	0.00	1.00
TPM1uf+I+G	6850.88	177	14990.44	26.70	0.00	1.00
TPM3uf+I	6854.83	176	14991.07	27.33	0.00	1.00
TIM1+I+G	6849.49	178	14994.94	31.20	0.00	1.00
TIM3+I	6853.24	177	14995.17	31.43	0.00	1.00
TVM+I	6849.67	178	14995.31	31.57	0.00	1.00
GTR+I	6848.00	179	14999.25	35.51	0.00	1.00
TPM2uf+I	6859.96	176	15001.33	37.59	0.00	1.00
HKY+I	6864.07	175	15002.26	38.52	0.00	1.00
TIM2+I	6858.26	177	15005.21	41.47	0.00	1.00
K80+G	6876.61	172	15005.50	41.76	0.00	1.00
TPM3+G	6873.36	173	15006.29	42.55	0.00	1.00
TrN+I	6862.51	176	15006.41	42.68	0.00	1.00
K80+I+G	6873.63	173	15006.81	43.08	0.00	1.00
TPM3+I+G	6870.38	174	15007.60	43.86	0.00	1.00
TPM1uf+I	6863.76	176	15008.91	45.18	0.00	1.00
TPM1+G	6875.85	173	15011.26	47.52	0.00	1.00
TrNef+G	6876.18	173	15011.93	48.19	0.00	1.00
TPM1+I+G	6872.68	174	15012.20	48.47	0.00	1.00
TPM2+G	6876.54	173	15012.64	48.91	0.00	1.00
TIM3ef+G	6872.94	174	15012.72	48.98	0.00	1.00
TIM1+I	6862.28	177	15013.25	49.52	0.00	1.00
TrNef+I+G	6873.27	174	15013.39	49.65	0.00	1.00
TPM2+I+G	6873.52	174	15013.89	50.15	0.00	1.00
TIM3ef+I+G	6869.91	175	15013.95	50.21	0.00	1.00

TIM1ef+G	6875.42	174	15017.68	53.95	0.00	1.00
TIM1ef+I+G	6872.21	175	15018.54	54.80	0.00	1.00
TVMef+G	6872.27	175	15018.66	54.92	0.00	1.00
TIM2ef+G	6876.12	174	15019.08	55.34	0.00	1.00
TVMef+I+G	6869.05	176	15019.50	55.77	0.00	1.00
TIM2ef+I+G	6873.06	175	15020.24	56.51	0.00	1.00
SYM+G	6871.85	176	15025.10	61.36	0.00	1.00
SYM+I+G	6868.59	177	15025.86	62.12	0.00	1.00
K80+I	6892.58	172	15037.44	73.70	0.00	1.00
TPM3+I	6889.00	173	15037.55	73.82	0.00	1.00
TPM1+I	6891.71	173	15042.98	79.24	0.00	1.00
TIM3ef+I	6888.42	174	15043.67	79.94	0.00	1.00
TrNef+I	6892.23	173	15044.01	80.28	0.00	1.00
TPM2+I	6892.44	173	15044.45	80.71	0.00	1.00
TIM1ef+I	6891.14	174	15049.13	85.39	0.00	1.00
TVMef+I	6887.70	175	15049.52	85.79	0.00	1.00
TIM2ef+I	6891.88	174	15050.61	86.87	0.00	1.00
SYM+I	6887.12	176	15055.64	91.90	0.00	1.00
F81+G	6931.81	174	15130.46	166.73	0.00	1.00
F81+I+G	6932.11	175	15138.34	174.60	0.00	1.00
JC+G	6954.45	171	15153.90	190.16	0.00	1.00
F81+I	6945.08	174	15157.01	193.27	0.00	1.00
JC+I+G	6955.38	172	15163.04	199.31	0.00	1.00
TPM3uf	6948.84	175	15171.81	208.07	0.00	1.00
TVM	6943.77	177	15176.21	212.48	0.00	1.00
TIM3	6948.29	176	15177.98	214.24	0.00	1.00
GTR	6943.17	178	15182.30	218.56	0.00	1.00
JC+I	6970.40	171	15185.79	222.05	0.00	1.00
TPM2uf	6956.76	175	15187.64	223.90	0.00	1.00
HKY	6960.49	174	15187.82	224.09	0.00	1.00
TIM2	6956.10	176	15193.60	229.86	0.00	1.00
TrN	6959.87	175	15193.87	230.13	0.00	1.00
TPM1uf	6960.14	175	15194.40	230.66	0.00	1.00
TIM1	6959.54	176	15200.48	236.75	0.00	1.00
TPM3	6987.80	172	15227.89	264.15	0.00	1.00
K80	6993.01	171	15231.01	267.27	0.00	1.00
TIM3ef	6987.64	173	15234.83	271.10	0.00	1.00
TPM1	6991.78	172	15235.85	272.11	0.00	1.00
TPM2	6992.77	172	15237.82	274.08	0.00	1.00
TrNef	6992.87	172	15238.02	274.29	0.00	1.00
TVMef	6985.82	174	15238.48	274.74	0.00	1.00
TIM1ef	6991.59	173	15242.74	279.01	0.00	1.00
TIM2ef	6992.58	173	15244.71	280.98	0.00	1.00
SYM	6985.65	175	15245.43	281.69	0.00	1.00
F81	7034.17	173	15327.89	364.16	0.00	1.00
JC	7061.49	170	15360.71	396.97	0.00	1.00

Table S4. D_{xy} between paralogs

	par5	par1	par2	par3a	par3b	par4
par5						
par1	0.306					
par2	0.374	0.0921				
par3a	0.307	0.0752	0.122			
par3b	0.304	0.0769	0.111	0.0169		
par4	0.281	0.046	0.0987	0.0759	0.07789	

Table S5. Pairwise comparisons of K_a/K_s ratios between paralogs (par) for each domain of the gene. SP: signal peptide; PR: propiece; BRICHOS: BRICHOS domain, AMP: Antimicrobial Peptide mature domain. M refers to monomorphic sequences: no genetic diversity can be depicted for the pairwise comparison.

Region	Domain	Paralog	Paralog					
5’	SP		par5	par1	par2	par3a	par3b	par4
		par5						
		par1	1.5842					
		par2	0.3786	0.8005				
		par3a	0.3597	0.7612	0			
		par3b	0.3597	0.7612	0	0		
		par4	0.7772	0.7612	0	0	0	
	PR		par5	par1	par2	par3a	par3b	par4
		par5						
		par1	1.5667					
		par2	1.9158	0.858				
		par3a	1.3084	0.2798	0.3757			
		par3b	1.0855	0.3998	0.4868	1.4101		
		par4	0.9976	0.327	0.492	0.252	0.5152	
3’	BRICHOS		parE	parA	parB	parC	parD	
		parE						
		parA	0.5741					
		parB	1.8245	0.214				
		parC	0.5629	0.4216	0.8065			
		parD	0.8603	0.8649	1.8177	0.2782		
	AMP		parE	parA	parB	parC	parD	
		parE						
		parA	M					
		parB	M	M				
		parC	M	M	M			
		parD	M	M	M	M		

Table S6. Log-likelihood values and parameter estimates for the BRICHOS domain region and the propiece of the preproalvinellacin gene. Maximum-likelihood models implemented in the codeML program of the PAML package for models that allow positive selection (M2, M3,M8) and those that do not (M0, M1, M7). M0, one-ratio; M1, neutral; M2, selection; M3, discrete; M7, β; M8, β+ω and the estimated log-likelihood values (l) by the codeml program, ω = dN/dS nonsynonymous/synonymous rate ratio; p = proportion of sites for each site class. M0: one estimated ω for all sites; M1a: estimate p_0 = proportion of sites with ω_0 = 0,p_1 = 1 - p_0, proportion of sites with ω_1 = 1; M2a: estimate p_0 (ω_0 = 0), p_1 (ω_0 = 1), and ω_2, p_2 = 1 - p_0 - p_1. M3: estimate p_0, p_1, ω_0, ω_1, and ω_2; p_2 = 1 - p_0 - p_1. M7: estimates p and q (parameters of β distribution of ω between 0 and 1). M8: same as M7 except additional site class where an estimated ω is allowed. Positively Selected Sites: Codon positions predicted to be under positive selection with a posterior probability of ** >0.99 and *>95% (identification of sites exhibiting dn/dS ratio >1). Sites refer to amino acids positions from the first M. *: P>95%; **: P>99 in the Naive Empirical Bayes (NEB) analyses of PAML.

Model		M0	M3 (Discrete)	M1 (Neutral)	M2 (Selection)	M7 (β)	M8 (β+ω)
BRICHOS	**Log likelihood**	-443.76	-437.09	-439.14	-437.09	-439.17	-437.09
	Parameters estimates	ω= 0,612	ω0=0, p0=0.79, ω1=2.78772 p1=0.18, ω2=2.78775 p2=0.03	ω0= 0, p0=0.67, (ω1=1) p1=0.33	ω0=0, p0=0.79, ω1=1 p1=0, ω2=2.78 p2=0.21	p=0.005, q=0.0117	p0=0.78, p=0.005, p1=0.21, q= 2.74, ω=2.78
	Sites with dN/dS>1 (NEB analysis)	n.a.	D119G; Q121H; N129S; T131I; D133G; D141E; V169A (all **)	n.a.	D119G; Q121H; N129S; T131I; D133G; D141E; V169A (all **)	n.a.	D119G; Q121H; N129S; T131I; D133G; D141E; V169A (all **)
	Sites with dN/dS>1 (BEB analysis)	n.a.	n.a.	n.a.	Q121H; N129S; D133G; D141E; V169A (not significant)	n.a.	Q121H; N129S; D133G; D141E; V169A (not significant)
PROPIECE	**Log likelihood**	-593.27	-585.85	-591.82	-585.88	-592.88	-585.88
	Parameters estimates	ω=1.2438 5	ω0=0.49, p0=0.76, ω1=3.33 p1=0.14, ω2=7.32 p2=0.1	ω0= 0, p0=0.29, (ω1=1) p1=0.71	ω0=0.45, p0=0.61, ω1=1 p1=0.21, ω2=5.96 p2=0.18	p=0.012, q=0.005	p0=0.81, p=5.23, p1=0.19, q= 3.99, ω=5.85
	Sites with dN/dS>1 (NEB analysis)	n.a.	N22I; W24R; L26Q; N30S; A31V; H33D*; P38YS*; D57E; T60IAS**; Q68E*; H76RD; L78S	n.a.	W24R; L26Q; N30S; H33D*; P38YS*; D57E; T60IAS**; Q68E*; H76RD; L78S	n.a.	N22I; W24R; L26Q; N30S; A31V; H33D*; P38YS*; D57E; T60IAS**; Q68E*; H76RD; L78S
	Sites with dN/dS>1 (BEB analysis)	n.a.	n.a.	n.a.	W24R; L26Q; N30S; H33D; P38YS;T60IAS*; Q68E*; H76RD	n.a.	W24R; L26Q; N30S; H33D; P38YS;T60IAS*; Q68E*; H76RD; L78S

Table S7. Statistical likelihood ratio tests comparing substitution models on BRICHOS and Propiece sequences. The deviances (LRT) calculated from paired CodeML models are compared with the critical values of chi-square asymptotic distribution with appropriate degrees of freedom.

BRICHOS		**Models**		
		M0 versus M3	**M1 versus M2**	**M7 versus M8**
	deviance	13.32	4.1	4.16
	df	4	2	2
	p-value	**0.0357**	0.1287	0.1249
PROPIECE		**Models**		
		M0 versus M3	**M1 versus M2**	**M7 versus M8**
	deviance	14.84	11.88	14
	df	4	2	2
	p-value	**0.0005**	**0.0026**	**0.0009**

References

1 Tasiemski, A. *et al.* Characterization and function of the first antibiotic isolated from a vent organism: the extremophile metazoan *Alvinella pompejana*. *PLoS ONE* **9**, e95737, doi:10.1371/journal.pone.0095737 (2014).

2 Plouviez, S., Le Guen, D., Lecompte, O., Lallier, F. H. & Jollivet, D. Determining gene flow and the influence of selection across the equatorial barrier of the East Pacific Rise in the tube-dwelling polychaete Alvinella pompejana. *BMC Evol Biol* **10**, 220, doi:10.1186/1471-2148-10-220 (2010).

3 Smith, J. M. Analyzing the mosaic structure of genes. *J Mol Evol* **34**, 126-129 (1992).

4 Huson, D. H. & Bryant, D. Application of phylogenetic networks in evolutionary studies. *Mol Biol Evol* **23**, 254-267, doi:10.1093/molbev/msj030 (2006).

5 Nielsen, R. Molecular signatures of natural selection. *Annu Rev Genet* **39**, 197-218, doi:10.1146/annurev.genet.39.073003.112420 (2005).

6 Yang, Z. & Bielawski, J. P. Statistical methods for detecting molecular adaptation. *Trends Ecol Evol* **15**, 496-503 (2000).

7 Parmakelis, A. *et al.* Anopheles immune genes and amino acid sites evolving under the effect of positive selection. *PLoS One* **5**, e8885, doi:10.1371/journal.pone.0008885 (2010).

8 Hahn, M. W. Distinguishing Among Evolutionary Models for the Maintenance of Gene Duplicates. *Journal of Heredity* **100**, 605-617, doi:10.1093/jhered/esp047 (2009).